

Near-Field Diffraction Imaging from Multiple Detection Planes

L Loetgering*, M Golembusch, R Hammoud, T Wilhein

Institute for X-Optics, RheinAhrCampus Remagen - Joseph-Rovan-Allee 2, 53424 Remagen, Germany

*loetgering@hs-koblenz.de

Abstract. We present diffraction imaging results obtained from multiple near-field diffraction constraints. An iterative phase retrieval algorithm was implemented that uses data redundancy achieved by measuring near-field diffraction intensities at various sample-detector distances. The procedure allows for reconstructing the exit surface wave of a sample within a multiple constraint satisfaction framework neither making use of a priori knowledge as enforced in coherent diffraction imaging (CDI) nor exact scanning grid knowledge as required in ptychography. We also investigate the potential of the presented technique to deal with polychromatic radiation as important for potential application in diffraction imaging by means of tabletop EUV and X-ray sources.

1. Introduction

With the construction of high-coherent flux synchrotron sources and the development of fast and high-capacity computation facilities, the X-ray community witnessed a recent advent of coherent imaging techniques [1]. A variety of different approaches has emerged that spans from single- to multi-shot data acquisition [2, 3]. While single-shot techniques such as CDI and holography principally allow for imaging fast processes [4], scanning techniques such as ptychography, where a specimen is translated transversal to a beam, allow to use redundant information to infer additional experimental parameters, such as illumination [5] and coherence [6]. Another technique that utilizes redundant information is propagation-based phase retrieval, where diffraction patterns are recorded at multiple sample-detector distances that may be used to provide multiple constraints for iterative phase retrieval algorithms [7].

We recently presented a technique [8] to overcome limited detector size and detector translation alignment in propagation-based phase retrieval using a coregistration approach that is reviewed in section 2. In this paper, we present experimental results on an extension of this technique to polychromatic illumination.

2. Algorithm

2.1. Algorithm

Multiple constraint satisfaction problems are conveniently described in a divide and conquer framework [9]. In the case of propagation-based phase retrieval, each recorded diffraction pattern provides a constraint that is imposed on the exit surface wave field by means of projection onto sets, i.e.



$$\pi_M(\psi) = \mathcal{D}_z^{-1} \left(\sqrt{I_z} \frac{\mathcal{D}_z(\psi)}{|\mathcal{D}_z(\psi)|} \right), \quad (1)$$

where ψ is the exit-surface wave field, \mathcal{D}_z is an angular spectrum near-field propagator and I_z is the intensity recorded at distance z from the sample. Given multiple diffraction intensities, the exit-surface wave can be updated via a weighted average of multiple projections

$$\psi^{n+1} = \frac{\sum_k c_k \pi_k(\psi^n)}{\sum_k c_k}, \quad (2)$$

where π_k denotes projection onto the k^{th} diffraction intensity constraint and c_k is a weighting factor (see subsection 2.2). The weighted average of projections in a three constraint satisfaction problem in two-dimensional Euclidean space is illustrated in Figure 1 on the left.

2.2. Coregistration procedure

The weighting factors in Equation 2 are the maxima of the normalized cross-correlation between the squared magnitude of the near-field propagated iterate and the measured intensity, i.e.

$$c_k(\Delta x, \Delta y) = \max \left\{ \frac{\iint I_k(x + \Delta x, y + \Delta y) |\mathcal{D}_z(\psi(x, y))|^2 dx dy}{\iint I_k(x, y) dx dy \iint |\mathcal{D}_z(\psi(x, y))|^2 dx dy} \right\}. \quad (3)$$

3. Experiment

3.1. Data acquisition

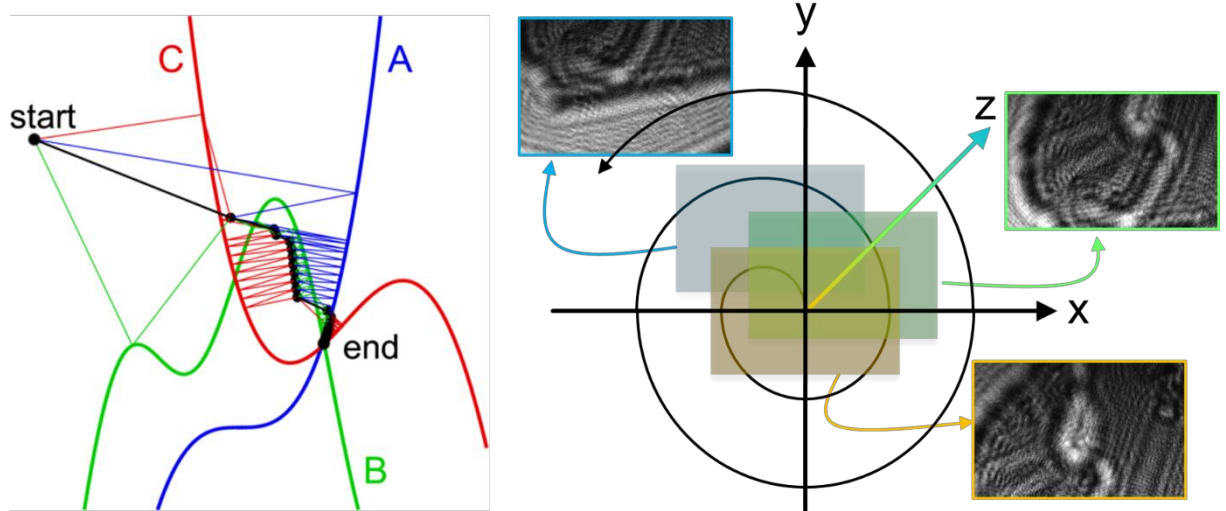


Figure 1 (left) illustration of the weighted average updating rule: Each iterate (black dots) is projected onto constraints A, B and C (colored curves) and then averaged to form the subsequent iterate, (right) the diffraction data is acquired along a screw spiralling around the optical axis.

To extend the numerical aperture of the detected data, the diffraction patterns were acquired in a spiralling motion along the optical axis, or in other words: the trajectory of each pixel on the detector prescribed a screw with extending diameter. The diffraction data was recorded on a UI-1226LE-M, 8 Bit CMOS detector with 480 x 752 pixels @ 6 μm . The detection geometry is shown on the right of Figure 1.

3.2. Monochromatic illumination

The left half of Figure 2 shows a reconstruction of a 10 μm thick histological section of a mouse brain. For this reconstruction 105 diffraction patterns were recorded (not shown here) at distances ranging from 100 mm to 308 mm ($\Delta z = 2$ mm) with an exposure time of 2 ms. The total lateral displacement of the detector was 123 mm in each transversal direction (2048 x 2048 pixels @ 6 μm). The light source used for plane wave illumination was an Argon-Ion-Laser with a wavelength of 488 nm. The reconstruction procedure was the same as described in [8].

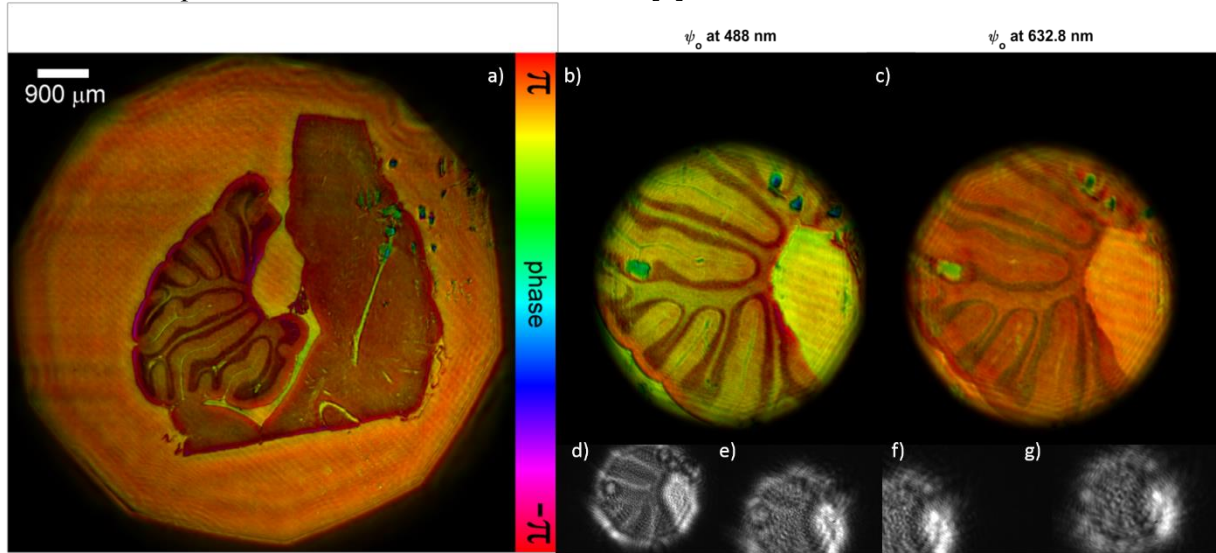


Figure 2 (a) propagation-based reconstruction of a mouse brain using monochromatic radiation at 488 nm, (b,c) polychromatic reconstructions of another slice of the mouse brain at 488 nm and 632 nm, respectively, (d-g) 4 out of 42 diffraction patterns used for the reconstruction of (b) and (c), transmissivity and phase shift of the specimen are encoded as brightness and hue, respectively.

3.3 Polychromatic illumination.

The right half of Figure 2 shows a polychromatic (488 nm and 632 nm) reconstruction of a similar slice of the same specimen as depicted in Figure 2a. Here a total of 42 diffraction patterns were recorded at distances 100 mm to 400 mm ($\Delta z = 5$ mm, exposure time 20 ms). The total lateral displacement of the detector was 24 mm in each transversal direction. The updating rule in Equation 1 had to be adapted to polychromatic radiation as proposed in [10], i.e.

$$\pi_M(\psi_l) = \mathcal{D}_z^{-1} \left(\frac{\sqrt{I_z} \cdot \mathcal{D}_z(\psi_l)}{\sqrt{\sum_l |\mathcal{D}_z(\psi_l)|^2}} \right), \quad (4)$$

where l is an index to label wavelength. For practical implementation it is noted that if the updating rule in Equation 2 converges slowly, initial updates can be implemented sequentially while for later iterations the averaged version in Equation 2 yields better photon statistics.

4. Discussion

4.1. Validity of the coregistration procedure

As pointed out in [8], the coregistration of adjacent diffraction patterns may fail if the detector is shifted too far along the optical axis. Shifting the detector within the longitudinal speckle size $l_z = 8\lambda(z/D)^2$, guarantees the wave field to exhibit a sufficient degree of temporal autocorrelation resulting in a reliable coregistration of diffraction patterns.

4.2. Requirements for polychromatic near-field reconstructions

For the polychromatic reconstruction depicted in Figure 2, an aperture was deliberately placed upstream the sample to limit the extent of the plane wave incident on the sample. This prevents the lowest spatial frequencies in the angular spectrum representation of the exit wave to overlap on a single pixel in the detector plane. Mathematically, this relation is expressed by $FOV \leq \Delta\lambda z/p$, where FOV is the field of view or the size of the aperture, $\Delta\lambda = \lambda_2 - \lambda_1$ is the wavelength separation of the two lasers and p is the pixel size of the detector. We believe that a similar relation holds for ptychographic information multiplexing [10].

5. Conclusion

Propagation-based phase retrieval does neither rely on a priori knowledge as required in CDI nor accurate mechanical scanning as required in ptychography. A disadvantage of propagation-based phase retrieval is that – without additional knowledge - it allows only to reconstruct the exit-surface wave emanating from the specimen as opposed to ptychography where both object transmission function and illumination can be retrieved.

Acknowledgment

L Loetgering would like to thank Prof. Dr. K Schilling from the Institute of Anatomy and Cell Biology at University of Bonn for the histological specimens.

References

- [1] Thibault P, Elser V 2010 *Annu. Rev. Condens. Matter Phys.* **1** 237-55.
- [2] Miao J, Charalambous P, Kirz J, Sayre D 1999 *Nature* **400** 342-4.
- [3] Rodenburg JM, Faulkner HM 2004 *Applied Physics Letters* **85** 4795-7.
- [4] Büttner F, Moutafis C, Schneider M, Krüger B, Günther CM, Geilhufe J, Schmising CV, Mohanty J, Pfau B, Schaffert S, Bisig A 2015 *Nature Physics* **11** 225-8.
- [5] Thibault P, Dierolf M, Menzel A, Bunk O, David C, Pfeiffer F 2008 *Science* **321** 379-82.
- [6] Thibault P, Menzel A 2013 *Nature* **494** 68-71.
- [7] Cloetens P, Ludwig W, Baruchel J, Van Dyck D, Van Landuyt J, Guigay JP, Schlenker M 1999 *Applied physics letters* **75** 2912-4
- [8] Loetgering L, Hammoud R, Juschkin L, Wilhein T 2015 *EPL (Europhysics Letters)* **111** 64002.
- [9] Gravel S, Elser V. 2008 *Physical Review E*. **78** 036706.
- [10] Batey DJ, Claus D, Rodenburg JM 2014 *Ultramicroscopy* **138** 13-21.